

Multiphoton ultraviolet spectroscopy of some $6p$ levels in krypton

Jeffrey Bokor*

Department of Electrical Engineering, Stanford University, Stanford, California 94305

Joshua (Yevsey) Zavelovich and Charles K. Rhodes

Department of Physics, University of Illinois at Chicago Circle, P.O. Box 4348, Chicago, Illinois 60680

(Received 6 November 1979)

The observation of two-photon excitation of selected $6p$ levels in krypton atoms using tunable ArF* laser radiation at 193 nm is reported. Using time-resolved detection of visible fluorescence lines in the vicinity of 430 nm arising from $6p-5s$ transitions, radiative lifetimes for the $6p[1/2]_0$ and $6p[3/2]_2$ states of 123 ± 5 and 115 ± 5 nsec, and collisional self-quenching rates of $(4.1 \pm 0.4) \times 10^{-10}$ cm³/sec and $(6.7 \pm 0.7) \times 10^{-10}$ cm³/sec, respectively, have been determined. By carefully measuring the visible fluorescence intensity as a function of incident laser intensity, the photoionization cross section of the $6p[3/2]_2$ state has been established as $(3.2 \pm 2.0) \times 10^{-19}$ cm². The two-photon transition rates for both states have been theoretically calculated, and good agreement is found with measurements of the relative excitation rates for the two transitions.

I. INTRODUCTION

Multiphoton spectroscopy is an extremely useful technique for studying the properties of excited states in atoms and molecules. Given an intense laser source, the technique allows one to obtain highly detailed information on states lying at excitation energies two, three, or more times the available laser photon energy. For example, with visible dye lasers, a wealth of information has been amassed on the properties of high-lying Rydberg states in atoms,¹ including level positions, fine structure and hyperfine structure, Zeeman and Stark effects, collisional mixing, and collisional quenching. Using carbon dioxide infrared lasers, high-resolution measurements have yielded accurate level positions for excited vibrational states of symmetric-top molecules, as well as pressure-broadening and pressure-shift data and vibrational transition matrix elements.² The recent advent of intense, tunable, ultraviolet excimer lasers has opened up a new region of the spectrum to detailed spectroscopic investigation via multiphoton absorption processes. Such laser systems have already been used to study collisional and radiative properties of the $E, F^1\Sigma_g^+$ state in molecular hydrogen³ and isotopic effects in two-photon photolysis of CO molecules.⁴ A number of other multiphoton spectroscopic and photochemical studies have also been carried out^{5,6} utilizing untuned excimer lasers.

In this study, we have used a tunable ArF* laser, operating at 193 nm, to excite discrete fine structure components of the $4p^56p$ configuration in Kr by a two-photon absorption process. The population densities of the excited states were monitored via

the $6p-5s$ fluorescence signals at ~ 430 nm. Using time-resolved spectroscopy, we have directly measured radiative decay lifetimes. Our results are compared with theoretical calculations,^{7,8} as well as other experimental measurements.^{7,9} In addition, we have obtained data on collisional deactivation of the excited atoms by ground-state krypton atoms. Our results are qualitatively comparable with those of Chang *et al.*,¹⁰ who studied collisional deactivation of $5p$ states in krypton in collisions with argon atoms.

As discussed in Refs. 3 and 5, often there is an important additional loss channel for electronically excited atomic and molecular systems excited by multiphoton ultraviolet absorption processes. This is due to excited-state photoionization by the intense ambient radiation field. As has been demonstrated in molecular hydrogen,³ this process may be studied in detail to yield numerical values for excited-state photoionization cross sections. In this manner, we have measured the cross section for photoionization of the $6p$ state in krypton at 193 nm. Hyman¹¹ has calculated photoionization cross sections for the $5p$ and $5s$ states in krypton and the $4p$ and $4s$ states in argon, while Dunning and Stebbings¹² have made measurements of the photoionization cross sections for metastable krypton ($5s^3P_{0,2}$) atoms. Our data for the $6p$ state in krypton may be qualitatively compared with these other results. A quantum-defect model of atomic photoionization¹³ may be used to estimate directly the $6p$ photoionization cross section. We also note that Stebbings, Dunning, and Rundel¹⁴ used a two-photon ionization technique to study photoionization of He ($np^1,^3P$) atoms which is, in many respects, quite similar to the one used here.

II. EXPERIMENTAL TECHNIQUE

The experimental arrangement used here is identical to that used in several similar studies.³⁻⁵ The output of a uv-preionized, discharge excited, rare-gas-halogen laser was focused by a 90-mm-focal-length calcium fluoride lens into a stainless-steel cell containing the sample under study. Cell pressure measurements were made using a capacitance manometer. The cell was capable of withstanding absolute pressures of up to 4 atm. Fluorescence was collected at right angles to the laser propagation direction by an *f*/1 magnesium fluoride lens and imaged onto the slit of a 0.3-m spectrometer equipped with an optical multichannel analyzer (OMA). For visible fluorescence detection, the spectrometer was equipped with a 1200 groove/mm grating blazed at 500 nm. The OMA was interfaced to a PDP 11/34 computer which was used for the data reduction and analysis. Time-resolved spectroscopic measurements were performed by replacing the OMA detector with a variable slit and a photomultiplier tube, converting the spectrometer to a standard monochromator configuration. The photomultiplier signal was processed by a transient digitizer which was also interfaced to the computer.

The ArF* laser was line narrowed and tuned by means of two high-quality fused silica prisms inserted in the laser cavity.¹⁵ This laser produced pulses of up to 30 mJ in energy at the peak of the tuning curve, with a 13-ns pulse duration. The laser bandwidth was 0.1 nm, and the effective tuning range was from 192.7–194.0 nm. The laser wavelength and linewidth were monitored during the experiments by a second 1-m spectrometer-OMA combination. Wavelength calibration was conveniently provided by the O₂ Schumann-Runge absorptions.¹⁶

III. TWO-PHOTON EXCITATION ESTIMATES

Figure 1 shows a partial energy level diagram for krypton, indicating the states which are involved in this experiment. Three sublevels of the $4p^56p$ configuration lie within the tuning range for two-photon excitation by the ArF* laser, namely $[\frac{1}{2}]_0$, $[\frac{3}{2}]_2$, and $[\frac{3}{2}]_1$. Here we use the *jl* coupling scheme notation, in which the orbital angular momentum \vec{l} of the excited electron is strongly coupled to the total angular momentum \vec{j} of the core, producing a resultant angular momentum \vec{k} . The spin \vec{s} of the excited electron is weakly coupled with \vec{k} to give the total angular momentum \vec{J} . Terms are designated by $nl [k]_J$ or $nl' [k]_{J'}$, corresponding to the $^2P_{1/2}$ and $^2P_{3/2}$ core states, respectively. These states may decay radiatively to $5s$ and $5s'$ states, emitting visible radiation.

The calculation of multiphoton transition probabilities has been a subject of intensive research in recent years, with particular attention having been paid to the effects of finite laser bandwidth and temporal coherence. The most recent and the most general theoretical treatment pertaining to the experimental situation at hand has been presented by Zoller.¹⁷ References to previous work may be found there. Zoller has examined the case of resonant multiphoton ionization by finite-bandwidth chaotic fields and gives the time evolutions of both the ionization probability and population density of the resonant bound state. When both the resonant bound-bound Rabi frequency and excited-state photoionization rate are much less than the laser bandwidth, a rate equation analysis is found to hold.¹⁷ All of the experiments reported here were carried out in this regime.

The two-photon transition rate is given by

$$W_{fg} \equiv \alpha I^2 / \hbar \omega = 2! \frac{(2\pi)^3}{(\hbar c)^2} I^2 |M_{fg}|^2 g(\omega). \quad (1)$$

This relation serves to define the two-photon coupling parameter α . With the incident laser intensity I given in W/cm², α has units of cm⁴/W. Appearing in (1) are the line-shape factor $g(\omega)$, which contains the dependence on the laser bandwidth, and the two-photon matrix element M_{fg} which is written in the form

$$M_{fg} = \sum_k \frac{\langle f | \hat{\epsilon} \cdot \vec{\mu} | k \rangle \langle k | \hat{\epsilon} \cdot \vec{\mu} | g \rangle}{E_{kg} - \hbar \omega}. \quad (2)$$

In this expression $\hat{\epsilon}$ denotes the polarization of the optical wave and $\vec{\mu}$ represents the electric operator. The atomic ground state is represented by $|g\rangle$ and the two-photon resonant bound state is represented by $|f\rangle$. The sum in Eq. (2) extends, in principle, over a complete set of intermediate states $|k\rangle$.

We now factor the dipole matrix elements appearing in (2), using the Wigner-Eckart theorem,¹⁸ in order to derive angular-momentum selection rules. The laser output may be taken to be linearly polarized, due to the presence of several Brewster angle-reflecting surfaces within the laser cavity. First consider the matrix element

$$\langle k | \hat{\epsilon} \cdot \vec{\mu} | g \rangle = (-1)^{J_k - M_k} \langle \gamma_k J_k || \mu || \gamma_g J_g \rangle \begin{pmatrix} J_k & 1 & J_g \\ -M_k & 0 & M_g \end{pmatrix}. \quad (3)$$

Here, the ground state is 1S_0 , hence $J_g = M_g = 0$. From the properties of the 3-*j* symbols,¹⁸ we immediately derive the selection rules $M_k = 0$, $J_k = 1$. With a similar factorization of the matrix element $\langle f | \hat{\epsilon} \cdot \vec{\mu} | k \rangle$, we obtain the selection rules on the final-state quantum numbers $M_f = 0$, $J_f = 0, 2$. The transition to $J_f = 1$ is forbidden, since

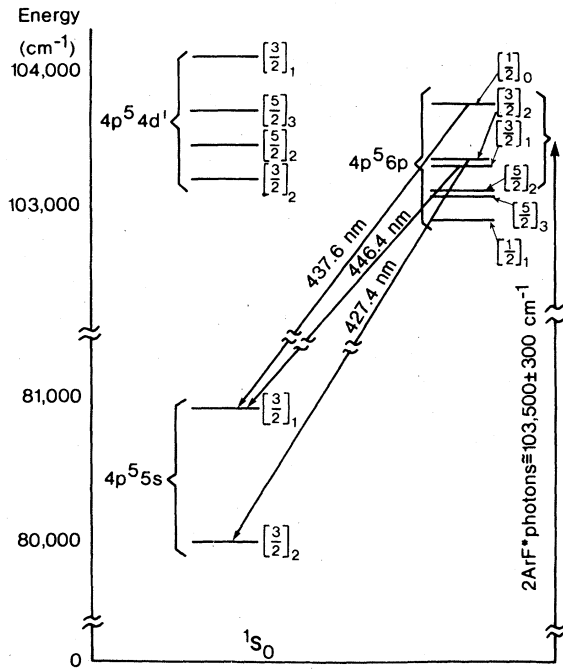


FIG. 1. Partial energy level diagram for krypton showing states excited by two-photon excitation and some radiative decay transitions of the excited states.

$$\begin{pmatrix} 1 & 1 & 1 \\ 0 & 0 & 0 \end{pmatrix} = 0. \quad (4)$$

Within the electric dipole approximation, these selection rules hold rigorously, regardless of how the summation in (2) is performed. We, therefore, expect to observe no direct excitation of the $6p[\frac{3}{2}]_1$ state by the linearly polarized laser radiation. With a circularly polarized, or unpolarized laser, of course, this state may also be excited.

In order to obtain order of magnitude estimates for the transition strengths to the $6p[\frac{1}{2}]_0$ and the $6p[\frac{3}{2}]_2$ states, we use the "single-path approximation," in which only one dominant intermediate state is considered, and the sum in expression (2) collapses to a single term. The appropriate state is $5s[\frac{3}{2}]_1$, which is the lowest excited state in Kr with the appropriate parity and total angular momentum. The dipole matrix element for the $5s[\frac{3}{2}]_1 - 4p^6(^1S_0)$ resonance transition may be derived from the measured oscillator strength for this transition¹⁹ of $f = 0.219$. The matrix elements for the $6p[\frac{1}{2}]_0 - 5s[\frac{3}{2}]_1$ and $6p[\frac{3}{2}]_2 - 5s[\frac{3}{2}]_1$ transitions are obtained by using our measured values for the $6p[\frac{1}{2}]_0 - 6p[\frac{3}{2}]_2$ radiative lifetimes (see Sec. IV) and previously measured radiative branching ratios.²⁰ On resonance, the line-shape factor $g(\omega)$ is given by^{5,17,21}

$$g(\omega) = \frac{0.939}{(2\Delta\omega_L^2 + \Delta\omega_D^2)^{1/2}}, \quad (5)$$

provided that the laser spectral intensity may be assumed to be Gaussian, with $\Delta\omega_L$ and $\Delta\omega_D$ representing the laser linewidth and two-photon transition Doppler width (FWHM), respectively. Using our measured laser linewidth of 25 cm^{-1} , and the intermediate state detuning value of $29\,000 \text{ cm}^{-1}$, we obtain the two-photon coupling parameters shown in Table I.

IV. EXPERIMENTAL RESULTS

In spite of the rather large bandwidth of our laser excitation source (25 cm^{-1}), it was possible to obtain completely selective excitation of the $6p[\frac{1}{2}]_0$ and $6p[\frac{3}{2}]_2$ states. As predicted in Sec. III, no excitation of the $6p[\frac{3}{2}]_1$ state was detected. Laser excitation spectra for the $6p[\frac{1}{2}]_0$ and $6p[\frac{3}{2}]_2$ states are shown in Fig. 2 for a Kr pressure of 26 torr. These plots represent time-integrated, fluorescence emission signals at 437.6 and 427.4 nm, respectively. The secondary peaks appearing in both spectra arise due to collisional intramultiplet energy transfer. The peak in Fig. 2(b) appears red shifted because it is off in the wing of the laser tuning range.

The time dependence of these emissions was investigated in order to extract radiative lifetimes and collisional quenching data. The laser frequency was adjusted to line center for the transition under study, and the monochromator was tuned to the appropriate visible emission wavelength. The decay rate for the visible fluorescence was then measured as a function of Kr pressure for pressures in the range 0–5 torr. The data obtained are shown in Fig. 3. For each data point in Fig. 3, the decay signals were averaged over 50 laser shots, and the decay rates were obtained from a linear least-squares fit to the log of the averaged fluorescence signal. Good fits were obtained using a single-exponential decay curve. The pseudo-first-order fluorescence decay rate is given by

$$-(1/t) \ln[N(t)/N(0)] = (\tau_{\text{rad}}^{-1} + k_q[\text{Kr}]). \quad (6)$$

Here, $N(t)$ is the number of excited atoms, τ_{rad} is the radiative lifetime of laser excited level, and

TABLE I. Estimates of two-photon excitation parameters for 6p states in Kr I.

State ($nl[k]j$)	Wavelength (nm)	μ_1 (debye)	μ_2 (debye)	α ($10^{-31} \text{ cm}^4/\text{W}$)
$6p[\frac{1}{2}]_0$	192.75	1.39	0.806	2.62
$6p[\frac{3}{2}]_2$	193.49	1.39	0.763	2.34

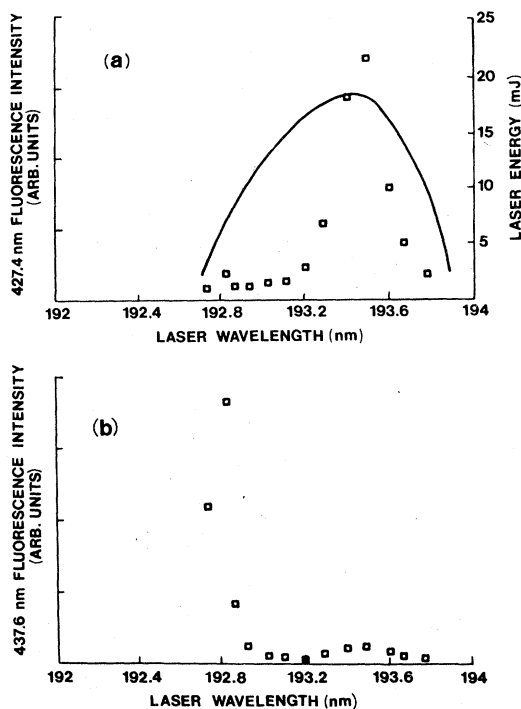


FIG. 2. Two-photon laser excitation spectra for krypton. (a) 427.4-nm fluorescence from $6p[3/2]_2$, (b) 437.6-nm fluorescence from $6p[1/2]_0$. The solid line in (a) is the laser output energy versus wavelength. Pressure in both cases is 26 torr.

k_q is the collisional self-quenching rate. The solid lines in Fig. 2 are linear least-squares fits of the data to the right-hand side of Eq. (6). The intercept gives the radiative decay constant τ_{rad}^{-1} , and the slope determines k_q .

The measured radiative lifetimes are listed in Table II, along with other experimental and theoretical results for comparison. For the $6p[3/2]_2$ level, our results are in good agreement with the measurements of Fonseca and Campos⁷ and the dipole velocity calculation of Gruzdev and Loginov.⁸ For the $6p[1/2]_0$ level, however, we find rather poor agreement with Fonseca and Campos, but again reasonable agreement with the dipole velocity

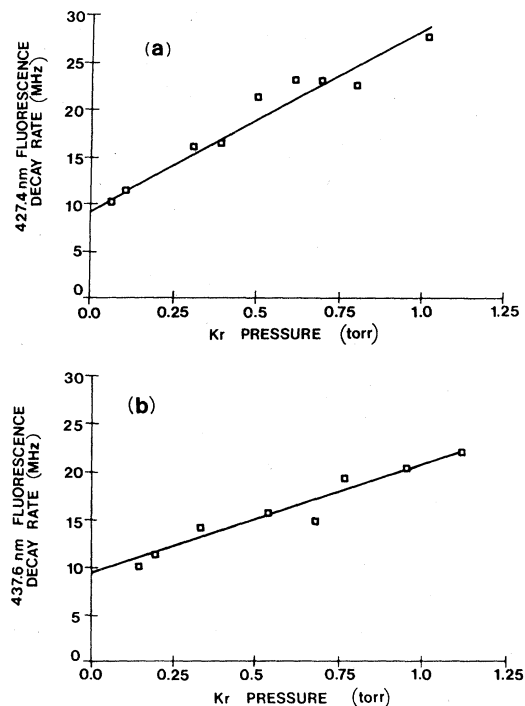


FIG. 3. Fluorescence decay rates for two-photon excited krypton. The squares are the experimental points. The solid lines are linear least-squares fits to the data. (a) 427.4-nm fluorescence from $6p[3/2]_2$ state. (b) 437.6-nm fluorescence from $6p[1/2]_0$ state.

calculation of Gruzdev and Loginov. We find poor agreement in both cases with the measurements⁹ of Delgado *et al.* Both previous experimental results utilized electron impact excitation and delayed coincidence detection. In those experiments, it was necessary to include at least two exponential terms in the data fits, in order to account for cascading effects. Due to the selective nature of our optical excitation method, such procedures are unnecessary, and a more direct measurement is obtained. Beyond this, the disagreement between the present results and previous experiments is not explained.

The measured self-quenching rates, obtained

TABLE II. Radiative lifetimes (in nanoseconds) for some $4p^56p$ levels in Kr I.

Level	Wavelength (nm)	This work	Fonseca and Campos ^a		Delgado <i>et al.</i> ^b	Gruzdev and Loginov ^c	
			Theory	Expt		μ_L	μ_v
$6p[1/2]_0$	437.6	123 ± 5	67.3	72 ± 3	74.3 ± 1	92.5	131
$6p[3/2]_2$	427.4	115 ± 5	80.4	118 ± 3	198 ± 4	79.8	117

^a Reference 7.

^b Reference 9: experimental values.

^c Reference 8: theoretical values; μ_L , results obtained using dipole length integrals; μ_v , results obtained using dipole velocity integrals.

from the data in Fig. 3 are for $6p[\frac{1}{2}]_0$, $k_q = (4.1 \pm 0.4) \times 10^{-10}$ cm³/sec, and for $6p[\frac{3}{2}]_2$, $k_q = (6.7 \pm 0.7) \times 10^{-10}$ cm³/sec. These states may quench by both intramultiplet and intermultiplet relaxation. Owing to the presence of the nearby $4d'$ states (see Fig. 1), these two processes are expected to be competitive.

To our knowledge, these are the first measurements of these particular collisional parameters in krypton. Our results are in qualitative agreement with the results of Chang and Setser²² for self-quenching of $3p$ states in neon and the results of Chang *et al.*¹⁰ for quenching of $5p$ states in krypton by ground-state argon atoms. In particular, rate constants for argon quenching of Kr($5p$) levels¹⁰ varied over the range $(0.05-3) \times 10^{-10}$ cm³/sec.

In addition to radiative decay and collisional quenching, there is an additional loss mechanism for the two-photon excited atoms, namely photoionization by the excitation laser. As shown in Ref. 3, this process may be exploited to yield numerical values for excited-state photoionization cross sections. The method involves making a careful measurement of the dependence of the two-photon excited fluorescence signal S on the excitation laser intensity I . In the absence of photoionization, S is expected to vary as I^2 . The photoionization loss modifies this behavior in a manner which we now describe.

We start from a simple rate equation analysis.¹⁷ With the excitation rates used here, ground-state depletion may be neglected. We, therefore, write

$$dN^*/dt = W_{fg}N_0 - N^*(\tau_{rad}^{-1} + k_q N_0 + \sigma_{pi} I/\hbar\omega). \quad (7)$$

Assuming a square pulse of length T_p , the solution to Eq. (7) is

$$N^*(t) = (\alpha I^2 N_0 / \hbar\omega B) (1 - e^{-Bt}), \quad 0 \leq t \leq T_p, \quad (8)$$

where the parameter B is defined as $B = \tau_{rad}^{-1} + k_q N_0 + \sigma_{pi} I/\hbar\omega$, and N_0 is the ground-state atom density. In many cases, the steady-state approximation $BT_p \gg 1$ holds, and we obtain

$$N^* = \frac{\alpha I^2}{\hbar\omega} N_0 \left(\tau_{rad}^{-1} + k_q N_0 + \frac{\sigma_{pi} I}{\hbar\omega} \right)^{-1}. \quad (9)$$

Since the fluorescent signal S is directly proportional to N^* , we see that the expected quadratic behavior of the fluorescent signal with I will saturate and go over to a linear behavior when

$$I > (\hbar\omega / \sigma_{pi}) (\tau_{rad}^{-1} + k_q N_0). \quad (10)$$

We rewrite Eq. (9) in the form

$$I/N^* = mI^{-1} + \beta, \quad (11)$$

and notice that

$$\sigma_{pi} = (\beta/m)\hbar\omega(\tau_{rad}^{-1} + k_q N_0)^{-1}. \quad (12)$$

The parameters β and m are derived from the experimentally measured dependence of the visible fluorescence signal S on the laser intensity I , and τ_{rad} and k_q have been experimentally determined as well, as described above. In this manner an experimental value for the cross section for photoionization of the two-photon excited level, at the wavelength of the excitation laser is obtained. Note that neither the absolute number of excited atoms produced, nor a value for the two-photon coupling parameter α are needed for this measurement. These parameters cancel out in the ratio β/m .

This procedure was carried out for $6p[\frac{3}{2}]_2$ level in krypton at 5 torr, and the results are shown in Fig. 4. The experimental points are plotted in the form of Eq. (11), and the solid line in the figure is a linear least-squares fit to the data. The result obtained by substituting the appropriate values into Eq. (12) is $\sigma_{pi} = (3.2 \pm 2.0) \times 10^{-19}$ cm². The major source of uncertainty in this experiment arises from the conversion of the measured laser output energy to the actual intensity at the laser focus. Since the laser output contains a large number of transverse modes, geometrical optics was used to estimate the dimensions of the focal spot. Most of our stated experimental uncertainty arises from uncertainty in this calculation. In addition, the actual temporal shape of the laser pulse deviates somewhat from the idealized square pulse assumed in the analysis of Eqs. (8)–(12). The rise and fall times of the laser pulse were measured to be each approximately 10% of the full pulse width. This introduces a systematic increase in the actual value of σ_{pi} above that calculated using the square pulse analysis, which is estimated to be in the range of 10–20%. This correction has been in-

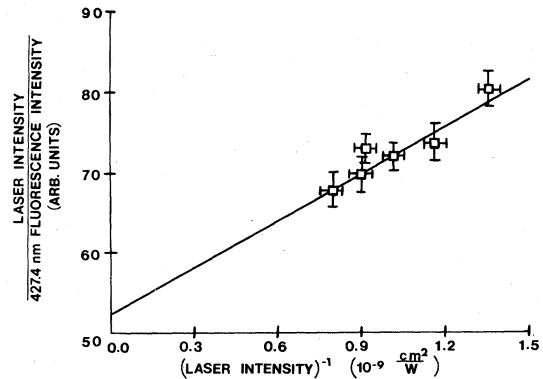


FIG. 4. Dependence of 427.4-nm fluorescence intensity on laser intensity plotted in the form of Eq. (11). The solid line is a linear least-squares fit to the data points.

corporated into the experimental value quoted above.

Photoionization of excited states in the rare gases has recently begun to receive attention in connection with the dynamics of rare-gas-halogen and rare-gas dimer laser systems. Hyman's calculations¹¹ for the first *s* and *p* excited states in krypton and argon indicate that losses due to the *p* level photoionization channel in these laser systems are significant. The experimental results of Dunning and Stebbings¹² support this theoretical result.

We know of no detailed calculations or other experimental results for photoionization of the $6p$ state in krypton. We may, however, compare our results with a simple quantum-defect approximation.^{13,23} We write the photoionization cross section for a given atomic level as²³ (in cm^2)

$$\sigma = \frac{8 \times 10^{-18}}{Z(U_I/R)^{1/2}(h\nu/U_I)^3} \quad (13)$$

In this expression, Z represents the net charge on the ion, U_I denotes the ionization potential for the atomic level in question, $h\nu$ is the incident photon energy, and R is the Rydberg constant. This formula is simply the exact expression¹³ for photoionization of hydrogenic atoms and thus represents a quantum-defect approximation for more complicated systems. This expression has been applied²³ to a variety of cases of excited-state photoionization for which experimental data already exist, including the rare gases.^{12,14} Remarkably good agreement is found, considering the simplicity of the model. Using this formula we obtain the cross section for photoionization of the $6p$ level in krypton at $\lambda = 193.5$ nm as $\sigma_{\text{pi}} = 1.8 \times 10^{-19} \text{ cm}^2$, which is in good agreement with the experimentally determined value.

With the important loss mechanisms characterized, it is now possible to test the theoretical two-photon absorption rates calculated in Sec. III against the observed signal strengths. Although our fluorescence detection sensitivity was not calibrated absolutely, we may compare the relative excitation strengths. At 9.5 torr pressure, the ratio of 437.6-nm fluorescence intensity to 427.4-nm fluorescence intensity when the $6p[\frac{1}{2}]_0$ and $6p[\frac{3}{2}]_2$ levels were excited at line center, respectively, was determined as 0.45. Using the two-photon coupling parameters derived in Sec. III, the measured laser energies of 3.5 and 8.5 mJ, and properly accounting for radiative to nonradiative branching and photoionization using our measured parameters (we assume equal photoionization cross sections for $6p[\frac{3}{2}]_2$ and $6p[\frac{1}{2}]_0$), we arrive at the predicted ratio of 0.42, in good agreement with the

experimental value. The closeness of this agreement is taken as support for the validity of the assumptions used in arriving at the predicted two-photon excitation rates.

V. CONCLUSIONS

Several multiphoton absorption processes have been observed in krypton atoms using ArF* laser excitation at 193 nm. Since the ArF* laser was tunable, a detailed spectroscopic investigation of the $6p[\frac{1}{2}]_0$ and $6p[\frac{3}{2}]_2$ states in krypton could be performed. These measurements furnished radiative lifetimes and collisional quenching rates for both states as well as the photoionization cross section of the $6p[\frac{3}{2}]_2$ state at 193 nm. The relative two-photon excitation rates for the two states have also been measured.

The results on radiative lifetimes are compared with other experimental and theoretical results. For the $6p[\frac{3}{2}]_2$ state, we find agreement with one of two alternative experimental values, while for the $6p[\frac{1}{2}]_0$ state, we are in clear disagreement with both of the other experimental values. The photoionization cross section determined for the $6p[\frac{3}{2}]_2$ level, when compared with a simple model of atomic photoionization, was found to exhibit good agreement. Finally, the data on the relative two-photon excitation rates conform well with rates calculated using a single path approximation.

It is clear, from expressions (1) and (5), that an enormous increase in excitation strength is to be gained by further narrowing the laser bandwidth. KrF* laser bandwidths better than 0.1 cm^{-1} have already been achieved²⁴ using injection locking techniques. ArF* laser linewidths on this order have also been achieved.²⁵ With such a laser, both the two-photon transition, and the photoionization process would saturate at a laser intensity of 10^{10} W/cm^2 with a laser fluence of 3–5 J/cm^2 . Such conditions would result in essentially full ionization of a sample of krypton atoms, and plasma densities of the order of 10^{16} cm^{-3} may be readily achieved in this manner.

ACKNOWLEDGMENTS

The authors wish to thank D. L. Huestis, R. M. Hill, R. T. Hawkins, and H. Egger for useful discussions involving various aspects of these experiments. We also thank D. W. Setser for communicating his results to us prior to publication. J. Bokor acknowledges the support of the Fannie and John K. Hertz Foundation. This work was supported by the Department of Energy under Agreement No. ED-78-S08-1603, the National Science Foundation under Grant No. PHY78-27610, and the Office of Naval Research under Contract No. N00014-78-C-0625.

- *Present address: Dept. of Physics, University of Illinois at Chicago Circle, P. O. Box 4348, Chicago, Ill. 60680.
- ¹For a recent review, see S. A. Edelstein and T. F. Gallagher, *Adv. At. Mol. Phys.* **14**, 365 (1978). See also N. Bloembergen and M. D. Levenson, in *High Resolution Laser Spectroscopy*, edited by K. Shimoda (Springer, Berlin, 1976), p. 315.
- ²J. Bokor, W. K. Bischel, and C. K. Rhodes, *J. Appl. Phys.* **50**, 4541 (1979); W. K. Bischel, P. J. Kelly, and C. K. Rhodes, *Phys. Rev. A* **13**, 1817 (1976); **13**, 1829 (1976).
- ³Daniel J. Kligler, Jeffrey Bokor, and Charles K. Rhodes, *Phys. Rev. A* **21**, 607 (1980).
- ⁴J. Bokor, J. Zavelovich, and C. K. Rhodes, *J. Chem. Phys.* **72**, 965 (1980).
- ⁵William K. Bischel, Jeffrey Bokor, Daniel J. Kligler, and Charles K. Rhodes, *IEEE J. Quantum Electron.* **QE-15**, 380 (1979).
- ⁶D. J. Kligler, H. Pummer, W. K. Bischel, and C. K. Rhodes, *J. Chem. Phys.* **69**, 4652 (1978); W. M. Jackson, Joshua B. Halpern, and Chung-San Lin, *Chem. Phys. Lett.* **55**, 254 (1978); A. P. Baronavski and J. R. MacDonald, *ibid.* **56**, 369 (1978); J. R. MacDonald, A. P. Baronavski, and V. M. Donnelly, *Chem. Phys.* **33**, 161 (1978); V. M. Donnelly and Louise Pasternack, *ibid.* **39**, 427 (1979).
- ⁷M. V. Fonseca and J. Campos, *Phys. Rev. A* **17**, 1080 (1978).
- ⁸P. F. Gruzdev and A. V. Loginov, *Opt. Spektrosk.* **38**, 611 (1975) [*Opt. Spectrosc. (USSR)* **38**, 1056 (1975)].
- ⁹A. Delgado, J. Campos, and C. Sanchez del Rio, *Z. Phys.* **257**, 9 (1972).
- ¹⁰B. Chang, H. Horiguchi, and D. Setser, *J. Chem. Phys.* (in press).
- ¹¹H. A. Hyman, *Appl. Phys. Lett.* **31**, 14 (1977).
- ¹²F. B. Dunning and R. F. Stebbings, *Phys. Rev. A* **9**, 2378 (1974).
- ¹³J. A. Gaunt, *Philos. Trans. R. Soc. London* **A229**, 163 (1930); H. A. Bethe and E. Salpeter, *Quantum Mechanics of One- and Two-Electron Atoms* (Academic, New York, 1957), p. 308.
- ¹⁴R. F. Stebbings, F. B. Dunning, and R. D. Rundel, in *Proceedings of the Fourth International Conference on Atomic Physics*, edited by G. zu Putlitz, E. W. Weber, and A. Wilmaker (Plenum, New York, 1975), p. 713.
- ¹⁵T. R. Loree, K. B. Butterfield, and D. L. Barker, *Appl. Phys. Lett.* **32**, 171 (1978).
- ¹⁶M. Ackerman and F. Biauame, *J. Mol. Spectrosc.* **35**, 73 (1970).
- ¹⁷P. Zoller, *Phys. Rev. A* **19**, 1157 (1979).
- ¹⁸A. R. Edmonds, *Angular Momentum in Quantum Mechanics* (Princeton University Press, Princeton, 1960).
- ¹⁹D. J. G. Irwin, J. A. Kernahan, E. H. Pinnington, and A. E. Livingston, *J. Opt. Soc. Am.* **66**, 1396 (1976).
- ²⁰W. F. Meggers, T. L. de Bruin, and C. J. Humphreys, *J. Res. Nat. Bur. Stand.* **7**, 643 (1931).
- ²¹B. R. Marx, J. Simons, and L. Allen, *J. Phys. B* **11**, L273 (1978).
- ²²R. S. F. Chang and D. W. Setser, *J. Chem. Phys.* (in press).
- ²³D. C. Lorents, D. J. Eckstrom, and D. L. Huestis, SRI International Report No. MP 73-2, Menlo Park, California, 1973 (unpublished).
- ²⁴J. R. Murray, J. Goldhar, and A. Szöke, *Appl. Phys. Lett.* **32**, 551 (1978); R. T. Hawkins, H. Egger, J. Bokor, and C. K. Rhodes, *Appl. Phys. Lett.* **36**, 391 (1980).
- ²⁵R. S. Hargrove and J. A. Paisner, in *Proceedings of the Topical Meeting on Excimer Lasers* (Optical Society of America, Charleston, 1979).